JOURNAL OF PROPULSION AND POWER
Vol. 18, No. 2, March–April 2002

Ethylene Ignition and Detonation Chemistry, Part 2: Ignition Histories and Reduced Mechanisms

B. Varatharajan* and F. A. Williams†
University of California, San Diego, La Jolla, California 92037-0417

The detailed mechanism of 148 steps among 34 chemical species that has been described previously is reduced through steady-state and partial-equilibrium approximations to achieve simplified descriptions for use in ignition and detonation studies. The concentration histories for ethylene oxidation reveal different types of ignition processes under not very different conditions of pressure and temperature. When unimportant steps are sequentially deleted from the detailed mechanism, a short mechanism is developed involving only 38 irreversible elementary steps among 21 chemical species. This short mechanism is designed to be applied with reasonable accuracy over the entire range of conditions indicated previously. If attention is restricted to the induction period, then these 38 steps can be decreased to 21. During induction, the important chain carriers are mainly H, O, OH, and C_2H_3 above 1500 K, whereas C_2H_3, HO_2, and H_2O_2 become dominant carriers below this temperature. At high temperatures, expressions for ignition time are derived by using radical depletion as the ignition criterion, whereas at lower temperatures, simplified thermal explosion theory in principle can be applied. Based on the detailed mechanism, a two-step mechanism involving only seven species is developed, which can facilitate computational investigations of multidimensional ignition and detonation processes of ethylene–air mixtures.

Introduction

THERE is limited overall understanding of the chemistry of ethylene ignition and detonation even though there are many chemical-kinetic descriptions available.[1–6] Reduced-chemistry descriptions can provide this overall understanding by decreasing the complexities of a large detailed mechanism through systematic application of steady-state and partial-equilibrium approximations. Some such descriptions are available for flame chemistry,[7] but none at all for ignition and detonation processes of ethylene. Recent investigations of acetylene[8] suggest that such overall understanding can provide expressions for ignition times and can lead to simplified chemical-kinetic descriptions that can be used in multidimensional computations of the structure and stability of real detonations. This second part of this two-part series on ethylene ignition and detonation is focused on developing an understanding of the overall chemistry of ignition and detonation of ethylene-air mixtures, starting with the detailed mechanism described in Part 1 (Ref. 9).

A short mechanism of 33 elementary steps, five reversible, among 21 chemical species is identified here from the detailed mechanism that has been described in Part 1. This mechanism yields ignition-time and subsequent heat-release predictions that are nearly as good as those of the full mechanism, and it facilitates detailed analyses of ignition histories that lead to identification of steady-state species and development of systematically reduced chemistry that addresses ignition with a small number of overall steps. Based on the reduced mechanism, an analytical expression for ignition time is derived for high-temperature conditions that compares well with predictions from the detailed mechanism. A simplified two-step mechanism is developed that can be used confidently in autoignition and detonation studies. Better understanding of ignition and detonation chemistry is thereby obtained.

Received 28 March 2001; revision received 26 July 2001; accepted for publication 30 July 2001.

*Graduate Student, Center for Energy Research, Department of Mechanical and Aerospace Engineering. Student Member AIAA.

†Professor and Director, Center for Energy Research, Department of Mechanical and Aerospace Engineering. Fellow AIAA.

Short Mechanism

Detailed chemical mechanisms of the type presented in Part 1, generally, contain many steps that are of little or no importance for predicting profiles of the chemical species of interest and temperature in particular applications. Simplifications, therefore, can be achieved by deleting steps that do not play a significant role. Such simplifications not only reduce computation times but also help in identifying the most important chemical paths. Although this kind of decrease in the number of elementary steps sometimes is called reduction of the mechanism, we call this process development of a short mechanism, reserving the term reduction for subsequent further simplification identifying overall steps through steady-state or partial-equilibrium approximations. The first criterion applied here for a short mechanism was that the resulting ignition times in air differ from those predicted by the detailed mechanism by less than 30%. The second criterion was that predicted temperatures during the subsequent heat-release period differ by less than 10%. These criteria were selected because ignition times and temperatures seldom can be measured more accurately.

Figure 1 shows a typical reaction-path diagram at an initial temperature of 1500 K and at a pressure of 1 bar, derived from the detailed mechanism. Such diagrams are helpful in identifying short mechanisms. The main oxidation path is seen in Fig. 1 to be the vinyl (C_2H_3) path that produces mainly both acetylene (C_2H_2), which is oxidized rapidly by O and OH attack, and the vinoxy (CH_2CHO) radical, which decomposes rapidly, producing H atoms and ketene (CH_2CO). The O attack on C_2H_4 is also important because both of its paths are chain branching, the path through methyl (CH_3) ultimately less so than that through vinoxy radicals. The H attack leading to the formation of C_2H_5 is unimportant at high temperatures, but it delays ignition significantly by removing H radicals at low temperatures (about 1000 K). Reactions involving methane and ethane lie to the side of the main ethylene ignition chains and, therefore, are not shown in Fig. 1. In addition, species involving three or more carbon atoms are relatively unimportant over the range of conditions addressed, as are the low-concentration species CH_2, CH, C_2H, HCCO, CH_3O, and CH_2OH. With steps leading to these species omitted, along with a number of radical–radical interactions, such as many of the direct three-body recombinations, that are unimportant because of low radical concentrations (and a few other slow or inconsequential steps), a short mechanism results that involves only 38 steps among 21 species, as given in Table 1, where the forward and backward steps are listed separately for the five

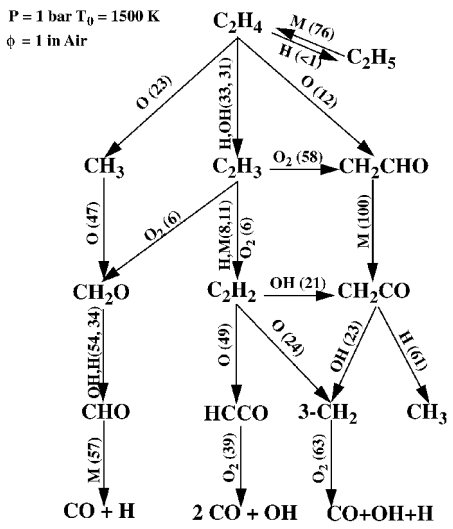

Fig. 1 Reaction-path diagram for the isobaric, adiabatic chemistry of a stoichiometric ethylene–air mixture, in homogeneous system at 1 bar and an initial temperature of 1500 K; percentages for each path are shown in parentheses.

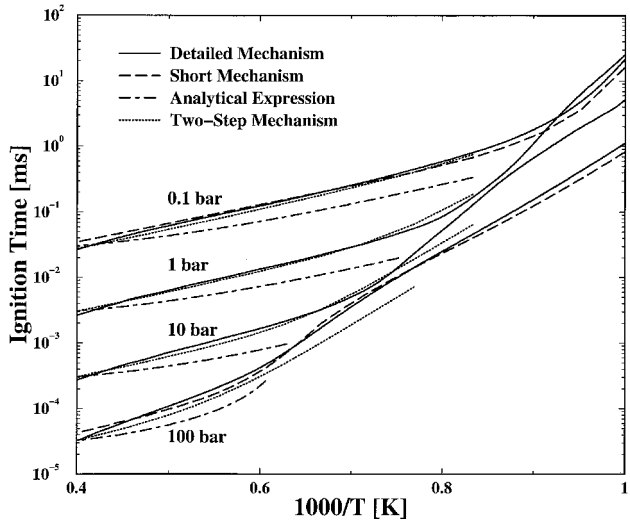

Fig. 2 Ignition-time comparison for predictions from detailed, short, and two-step mechanisms and from the analytical expression, for isobaric homogeneous ignition of stoichiometric ethylene–air mixtures.

steps that are reversible. This short mechanism is sufficient for most aspects of ethylene detonation. If, for example, profiles of chemiluminescence from CH radicals are required, then it is necessary to reinstate the steps leading to CH production and removal, but this will not appreciably affect other aspects of ignition histories.

The ignition-time predictions from this short mechanism agree remarkably well with those from the detailed mechanism. Representative comparisons, with inflection in the temperature–time trace employed as the ignition criterion, are shown in Fig. 2 for a wide range of temperatures and pressures, where the curves for the short mechanism for 1 and 10 bar, although in good agreement with those for the detailed mechanism, have been omitted for clarity, and the curves for the two-step mechanism and the analytical expression will be discussed later. Further comparisons of ignition-time predictions for different specific experiments have been mentioned in Part 1. Figure 3 offers more detailed comparisons between predictions of the ignition histories by showing temperature histories for an initial temperature of 1500 K and initial pressures of 0.1–100 bar. In addition, Fig. 4 shows comparisons between predictions of the detailed and the short mechanisms for the concentration histories at 1 bar and 1500 K. The curves in Figs. 3 and 4 demonstrate agreement within the criteria specified earlier, at least when the ignition

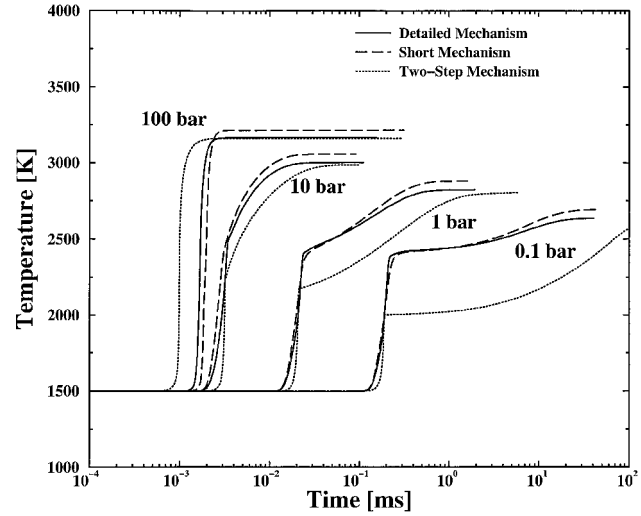

Fig. 3 Comparison between predictions of temperature histories from the detailed, short, and two-step mechanisms, for isobaric conditions in stoichiometric ethylene–air mixtures.

criteria are based on the temperature inflection. Figure 4 suggests similar agreement irrespective of the ignition criteria employed. For predicting ignition times, in fact, only steps 1, 6, 10, 11, 16, 17, 18, 19, 20, 21, 22, 23, 25, 26, 27, 29, 30, 31, 34, 35, and 38, involving 18 chemical species, are required; the 17 remaining steps are important for describing subsequent heat release after ignition.

Ignition Histories

Histories of temperatures and species concentrations during ignition were computed using FlameMaster.[10] As explained in part 1, the calculations were performed for homogeneous, adiabatic, isobaric conditions, but are quite representative of shock-tube experiments before significant heat release. Figure 5 shows resulting ignition histories of the most active radicals and temperature based on the detailed mechanism for four different initial temperatures at a pressure of 100 bar. These high-pressure conditions were chosen so that the entire range of different types of ignition phenomena could be exhibited conveniently; at lower pressures, the type of behavior seen here at 1000 K does not occur in the temperature range investigated (it does occur at temperatures below 1000 K).

Nearly isothermal chemistry followed by an abrupt temperature increase is evident for all initial temperatures in Fig. 5, although at high temperatures (2500 K) the induction period is noticeably endothermic. It is seen that, after the short initial increase in radical concentrations, there is an extended period during which the concentrations follow straight lines in Figs. 5, which indicates exponential growth with time. The initial increase is the initiation stage, and the exponential growth is the chain-branching stage of the ignition process. The slopes of the lines are equal for nearly all species during the chain-branching stage; it will be seen that this can be understood from the chemical mechanism, as can the few slopes that differ (see also Fig. 4). The chain branching occurs nearly isothermally and eventually is followed by a thermal runaway marking ignition. It is interesting to compare these histories with those found for ignition of other fuels. The chain-branching slopes resemble those found for acetylene ignition.[8] For methane ignition, there is a wider variety of different slopes for different species, as can be understood from the special nonlinear character of the chain-branching process of methane.[11] For both acetylene and methane, however, thermal runaway leading to ignition occurs at some time during the chain-branching stage and is responsible for the termination of this stage, in accord with the general theory of branched-chain thermal explosions.[12] Ethylene behaves differently, depending on the initial temperature, as may be seen most clearly in Fig. 5.

At lower temperatures, with the chosen kinetic mechanism, the chain-branching stage is terminated by an approximate leveling off that occurs through nearly isothermal chemical kinetics, resulting

Table 1 Short mechanism for C_2H_4 detonation

Number	Reaction	A[a]	n[a]	E[a]
	Hydrogen–oxygen chain			
1	$H + O_2 \rightarrow OH + O$	3.52×10^{16}	−0.70	71.4
2	$OH + O \rightarrow H + O_2$	1.15×10^{14}	−0.32	−0.7
3	$OH + H_2 \rightarrow H_2O + H$	1.17×10^{9}	1.30	15.2
4	$O + H_2O \rightarrow 2OH$	7.60×10^{0}	3.84	53.5
5	$2OH \rightarrow O + H_2O$	2.45×10^{-1}	3.97	−19.0
	Hydroperoxyl formation and consumption			
6[b]	$H + O_2 + M \rightarrow HO_2 + M$	2.60×10^{19}	−1.20	0.0
7	$HO_2 + H \rightarrow 2OH$	1.70×10^{14}	0.00	3.7
8	$HO_2 + H \rightarrow H_2 + O_2$	4.28×10^{13}	0.00	5.9
9	$HO_2 + OH \rightarrow H_2O + O_2$	2.89×10^{13}	0.00	−2.1
	Hydrogen peroxide formation and consumption			
10	$2HO_2 \rightarrow H_2O_2 + O_2$	3.02×10^{12}	0.00	5.8
11[c]	$H_2O_2 \rightarrow 2OH \quad k_0$	7.94×10^{24}	−2.21	212.0
	k_∞	2.55×10^{20}	−1.68	219.1
	Direct recombination			
12[b]	$H + OH + M \rightarrow H_2O + M$	2.20×10^{22}	−2.00	0.0
13[b]	$H_2O + M \rightarrow H + OH + M$	2.18×10^{23}	−1.93	499.0
	Carbon monoxide reactions			
14	$CO + OH \rightarrow CO_2 + H$	4.40×10^{6}	1.50	−3.1
15	$CO_2 + H \rightarrow CO + OH$	4.97×10^{8}	1.50	89.7
	Initiation and fuel consumption			
16	$C_2H_4 + O_2 \rightarrow C_2H_3 + HO_2$	4.22×10^{13}	0.00	241.0
17	$C_2H_4 + OH \rightarrow C_2H_3 + H_2O$	5.53×10^{05}	2.31	12.4
18	$C_2H_4 + O \rightarrow CH_3 + CHO$	2.25×10^{06}	2.08	0.0
19	$C_2H_4 + O \rightarrow CH_2CHO + H$	1.21×10^{06}	2.08	0.0
20	$C_2H_4 + HO_2 \rightarrow C_2H_4O + OH$	2.23×10^{12}	0.00	71.9
21	$C_2H_4 + H \rightarrow C_2H_3 + H_2$	4.49×10^{07}	2.12	55.9
22[d]	$C_2H_4 + H \rightarrow C_2H_5 \quad k_0$	1.90×10^{35}	−5.57	21.1
	k_∞	1.08×10^{12}	0.45	7.6
23[e]	$C_2H_4 + M \rightarrow C_2H_3 + H + M$	2.60×10^{17}	0.00	404.0
	Vinyl, methyl, vinoxy, and ethyl consumption			
24	$C_2H_3 + H \rightarrow C_2H_2 + H_2$	1.21×10^{13}	0.00	0.0
25	$C_2H_3 + O_2 \rightarrow CH_2O + CHO$	1.70×10^{29}	−5.31	27.2
26	$C_2H_3 + O_2 \rightarrow CH_2CHO + O$	7.00×10^{14}	−0.61	22.0
27	$CH_3 + O_2 \rightarrow CH_2O + OH$	3.30×10^{11}	0.00	37.4
28	$CH_3 + O \rightarrow CH_2O + H$	8.43×10^{13}	0.00	0.0
29	$CH_2CHO \rightarrow CH_2CO + H$	1.05×10^{37}	−7.19	186.0
30	$C_2H_5 + O_2 \rightarrow C_2H_4 + HO_2$	2.00×10^{12}	0.00	20.9
31[d]	$C_2H_5 \rightarrow C_2H_4 + H \quad k_0$	3.99×10^{33}	−4.99	167.4
	k_∞	1.11×10^{10}	1.04	153.8
	Ketene, formaldehyde, formyl, acetylene, and ethylene oxide consumption			
32	$CH_2CO + H \rightarrow CH_3 + CO$	1.11×10^{07}	2.00	8.4
33	$CH_2O + OH \rightarrow CHO + H_2O$	3.90×10^{10}	0.89	1.7
34[f]	$CHO + M \rightarrow CO + H + M$	1.86×10^{17}	−1.00	71.1
35	$CHO + O_2 \rightarrow CO + HO_2$	3.00×10^{12}	0.00	0.0
36	$CHO + H \rightarrow CO + H_2$	1.00×10^{14}	0.00	0.0
37	$C_2H_2 + OH \rightarrow CH_2CO + H$	1.90×10^{07}	1.70	4.2
38	$C_2H_4O + HO_2 \rightarrow CH_3 + CO + H_2O_2$	4.00×10^{12}	0.00	71.2

[a]Specific reaction-rate constant $k = AT^n e^{-E/RT}$; units mol, cm^3, s, K, and kJ/mol.
[b]Chaperon efficiencies: O_2, 0.3; H_2O, 7.0; CO, 0.75; CO_2, 1.5; C_2H_6, 1.5; Ar, 0.5; and others, 1.0.
[c]Troe falloff $F_c = 0.265\exp(-T/94) + 0.735\exp(-T/1756) + \exp(-5182/T)$. Chaperon efficiencies: H_2, 2.0; H_2O, 6.0; CO, 1.5; CO_2, 2.0; Ar, 0.7; and others, 1.0.
[d]Troe falloff $F_c = 0.832\exp(-T/1203)$ from Feng et al.[15]
[e]Chaperon efficiencies: 1.0, all.
[f]Chaperon efficiencies: CO, 2.5; CO_2, 2.5; H_2, 1.9; H_2O, 12.0; and others, 1.0.

in a period of nearly constant concentrations before thermal explosion. This constant-concentration stage can occupy an appreciable fraction of the total ignition time, particularly at the lowest temperatures considered, as seen in Fig. 5 at 1000 K. The presence of this additional stage is a complicating factor in ethylene ignition. It will be seen later that a reasonable criterion for the onset of the constant-concentration stage at the lower temperatures is achievement of an HO_2 steady state. At these low temperatures, HO_2 is initially formed rapidly through reaction 6 in Table 1, and it recombines in the constant-concentration stage to form H_2O_2, releasing heat and leading to thermal explosion. In a first approximation, then, ethylene ignition between 1000 and 1500 K can be viewed as a classical Frank–Kamenetskii thermal runaway (see Ref. 13), occurring in the mixture that is present in the constant-concentration stage of HO_2 steady state. Because the initiation stage is very short, the ignition time may then be viewed as the sum of the duration of the chain-branching stage and the classical thermal-runaway ignition time of the constant-concentration stage in this temperature range, but the separation of these two stages may not be sufficiently sharp for this view to yield an accurate ignition time.

As the initial temperature increases, concentrations of the radicals increase, while the duration of the constant-concentration stage decreases and is almost absent at 1500 K (Fig. 5). At these intermediate temperatures, H and C_2H_3 are formed in higher concentrations because of the increased rates of reactions 29 and 21, respectively, in Table 1. The species HO_2 is relatively unimportant under these high-temperature conditions, and the most important reactions are the exothermic O and OH attacks on C_2H_4. There is mild evidence

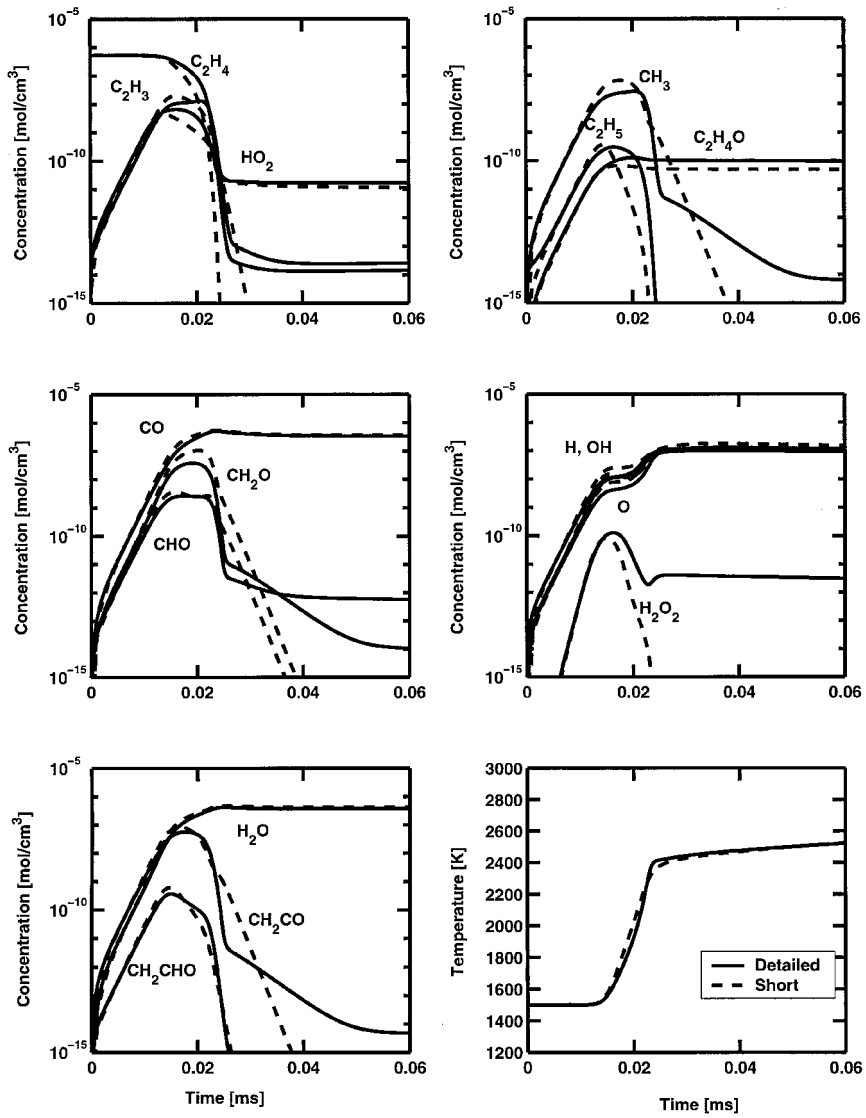

Fig. 4 Predicted concentration and temperature histories for adiabatic, isobaric evolution of stoichiometric ethylene–air mixtures at 1 bar and an initial temperature of 1500 K.

of chain-branching thermal explosion at these intermediate temperatures, as can be seen in Fig. 5 from the upward curvature of the radical profiles at 1500 K.

As temperature increases further, the rate of reaction 21 increases, and at an initial temperature of 2000 K, C_2H_3 is produced at a much more rapid rate. The increased importance of the H attack at these higher temperatures leads eventually to reactant depletion before the exothermic OH and O attacks can significantly influence ignition. Ignition under these high-temperature conditions is eventually due to the oxidation of vinyl through the exothermic reaction 25. Thus, at high temperatures, an accurate expression for ignition time can be obtained by identifying the time at which the concentration of C_2H_3 approaches the concentration of the fuel, marking the onset of reactant depletion.

At very high initial temperatures (above 2000 K), through reaction 23, thermal decomposition produces C_2H_3 and H directly, leading to ignition more rapidly. This initial endothermic decomposition contributes to the appreciable drop in temperature seen at early time in Fig. 5 at 2500 K, as does the endothermic decomposition to $C_2H_2 + H_2$, which is much faster but not included in the short mechanism because its effect on ignition time is negligible. The choice of reactant depletion as the ignition criterion continues to lead to reasonably accurate predictions under these conditions.

Ethylene, thus, exhibits a variety of ignition phenomena depending on the initial temperature and pressure. For obtaining simplified reduced mechanisms and expressions for the ignition time, it is important to examine carefully the various stages during the ignition process and to identify the important elementary reactions and steady-state species during those stages.

Induction-Zone Chemistry

In the induction zone, there is an initiation stage, a chain-branching stage, and, at low temperatures, a constant-concentration stage, as was seen in Fig. 5. These three stages are discussed in more detail in the Appendix. These stages are relevant for determining ignition times, for which 21 elementary steps among 18 species were identified previously as being sufficient for good agreement with predictions of the detailed mechanism. The induction-zone chemistry, thus, involves these 21 elementary steps. Computational complexity is characterized better by the number of independent species than by the number of elementary reactions, that is, by the number of independent differential equations involved. From this computational perspective, the induction-zone chemistry is of 13th order; in other words, from a reduced-chemistry viewpoint, the 21 elementary reactions define a 13-step mechanism. This is sufficiently complex that there is motivation to seek simplification through further approximation.

The induction period is nearly isothermal, and fuel and oxidizer concentrations do not change significantly during induction. The induction-zone problem, therefore, would be linear, except for the

Table 2 Short mechanism for ethylene ignition

No.	Reaction	Rate[a]
1	$H + O_2 \rightarrow p\ OH + p\ O + (1-p)\ HO_2$	$(\alpha_1 + \alpha_6)[H]$
11	$H_2O_2 \rightarrow 2OH$	$\alpha_{11}[H_2O_2]$
16	$C_2H_4 + O_2 \rightarrow C_2H_3 + HO_2$	$\alpha_{16}[C_2H_4]$
17	$C_2H_4 + OH \rightarrow C_2H_3 + H_2O$	$\alpha_{17}[OH]$
18	$C_2H_4 + O \rightarrow q\ CH_3 + q\ CHO + (1-q)\ CH_2CHO + (1-q)\ H$	$(\alpha_{18} + \alpha_{19})[O]$
20	$C_2H_4 + 2HO_2 \rightarrow CH_3 + CO + H_2O_2 + OH$	$\alpha_{20}[HO_2]$
21	$C_2H_4 + H \rightarrow r\ C_2H_3 + r\ H_2 + (1-r)\ C_2H_5$	$(\alpha_{21} + \alpha_{22})[H]$
25	$C_2H_3 + O_2 \rightarrow s\ CH_2O + s\ CHO + (1-s)CH_2CHO + (1-s)\ O$	$(\alpha_{25} + \alpha_{26})[C_2H_3]$
27	$CH_3 + O_2 \rightarrow CH_2O + OH$	$\alpha_{27}[CH_3]$
29	$CH_2CHO \rightarrow CH_2CO + H$	$\alpha_{29}[CH_2CHO]$
30	$C_2H_5 + t\ O_2 \rightarrow C_2H_4 + t\ HO_2 + (1-t)\ H$	$(\alpha_{30} + \alpha_{31})[C_2H_5]$
34	$CHO + (1-u)\ O_2 \rightarrow CO + u\ H + (1-u)\ HO_2$	$(\alpha_{34} + \alpha_{35})[CHO]$

[a]Rate constant $\alpha_1 = k_1[O_2]$, $\alpha_6 = k_6[O_2][M]$, $\alpha_{11} = k_{11}$, $\alpha_{16} = k_{16}[O_2]$, $\alpha_{17} = k_{17}[C_2H_4]$, $\alpha_{18} = k_{18}[C_2H_4]$, $\alpha_{19} = k_{19}[C_2H_4]$, $\alpha_{20} = k_{20}[C_2H_4]$, $\alpha_{21} = k_{21}[C_2H_4]$, $\alpha_{22} = k_{22}[C_2H_4]$, $\alpha_{25} = k_{25}[O_2]$, $\alpha_{26} = k_{26}[O_2]$, $\alpha_{27} = k_{27}[O_2]$, $\alpha_{29} = k_{29}$, $\alpha_{30} = k_{30}[O_2]$, $\alpha_{31} = k_{31}$, $\alpha_{34} = k_{34}[M]$, and $\alpha_{35} = k_{35}[O_2]$.

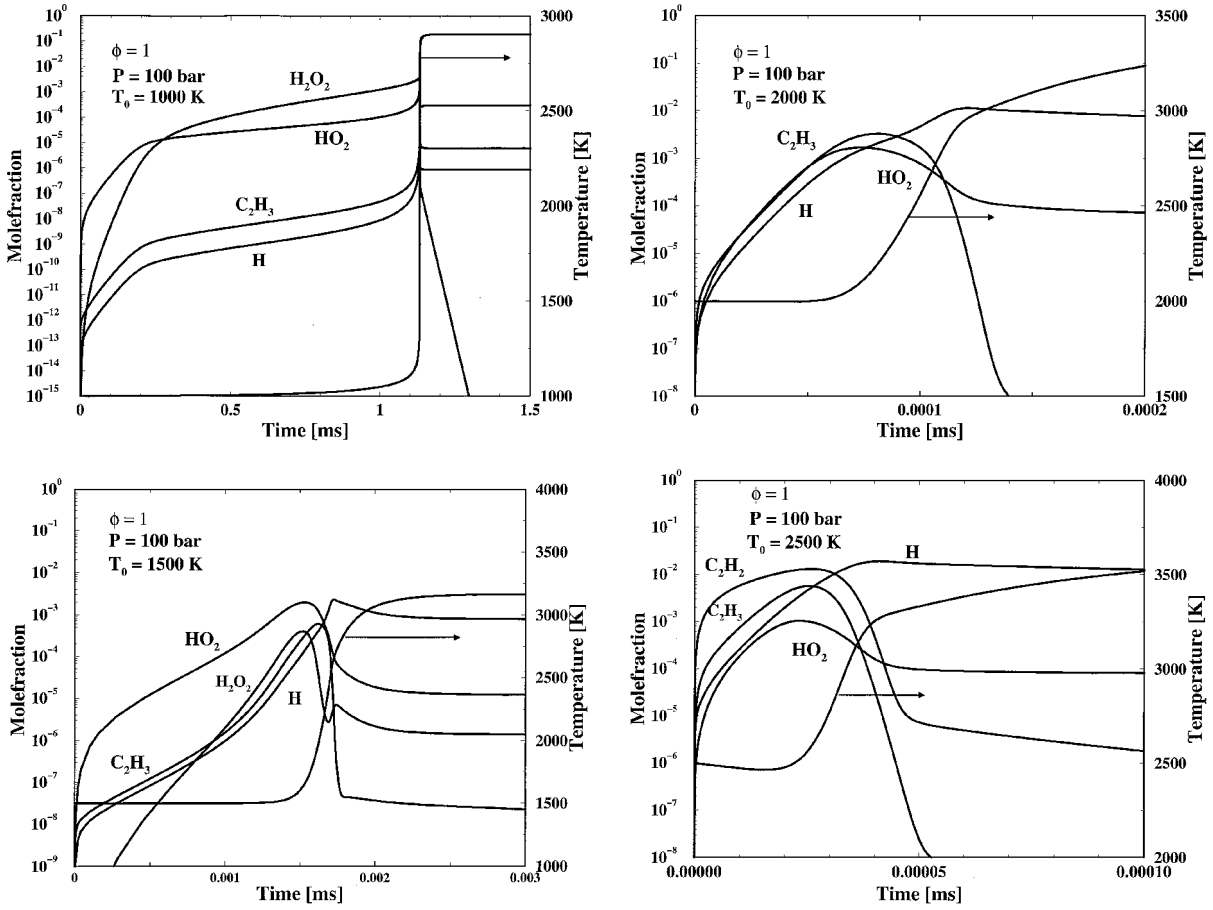

Fig. 5 Concentration and temperature histories for ignition of stoichiometric ethylene–air mixtures in an isobaric homogeneous reactor for four different conditions, from the detailed mechanism.

occurrence of reactions 10 and 38, each between two intermediaries, important only at the lower temperatures of interest. Without excessive error, for simplicity, reaction 10 can be neglected initially during initiation, and a steady-state approximation can be introduced for ethylene oxide because of its low concentration during induction, so that reaction 20 effectively becomes $C_2H_4 + 2HO_2 \rightarrow CH_3 + CO + H_2O_2 + OH$ overall. This produces a linear system and, by eliminating C_2H_4O, reduces the system to 12th order. Further neglecting reaction 23, which is of importance only at the highest temperatures, we obtain the 12-step short linear reduced mechanism of Table 2.

In Table 2, as well as for further analysis, it proves convenient to define equivalent first-order rate constants α_i, where i refers to the reaction number in Table 1. These constants have units of reciprocal seconds and refer to the inverse of the characteristic times for each of these reactions. The constant fuel and oxidizer concentrations, along with the constant elementary rate constants k_i for each reaction, are used in defining these constant α_i, which are given explicitly in the footnote to Table 2. In terms of these α_i, the nondimensional parameters

$$p = \frac{\alpha_1}{\alpha_1 + \alpha_6}, \qquad q = \frac{\alpha_{18}}{\alpha_{18} + \alpha_{19}}, \qquad r = \frac{\alpha_{21}}{\alpha_{21} + \alpha_{22}}$$

$$s = \frac{\alpha_{25}}{\alpha_{25} + \alpha_{26}}, \qquad t = \frac{\alpha_{30}}{\alpha_{30} + \alpha_{31}}, \qquad u = \frac{\alpha_{34}}{\alpha_{34} + \alpha_{35}} \quad (1)$$

can be defined. These parameters refer to the branching ratios and typically are functions of pressure and temperature, as seen in

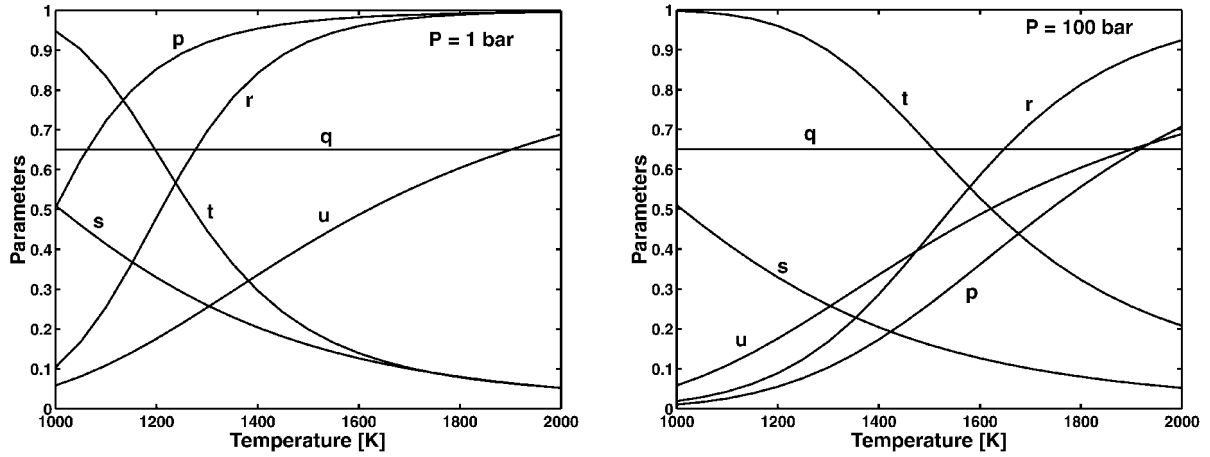

Fig. 6 Temperature and pressure dependence of the parameters p, q, r, s, t, and u; $[O_2]/[M] = 0.2$, stoichiometric in air, employed for the t and u curves.

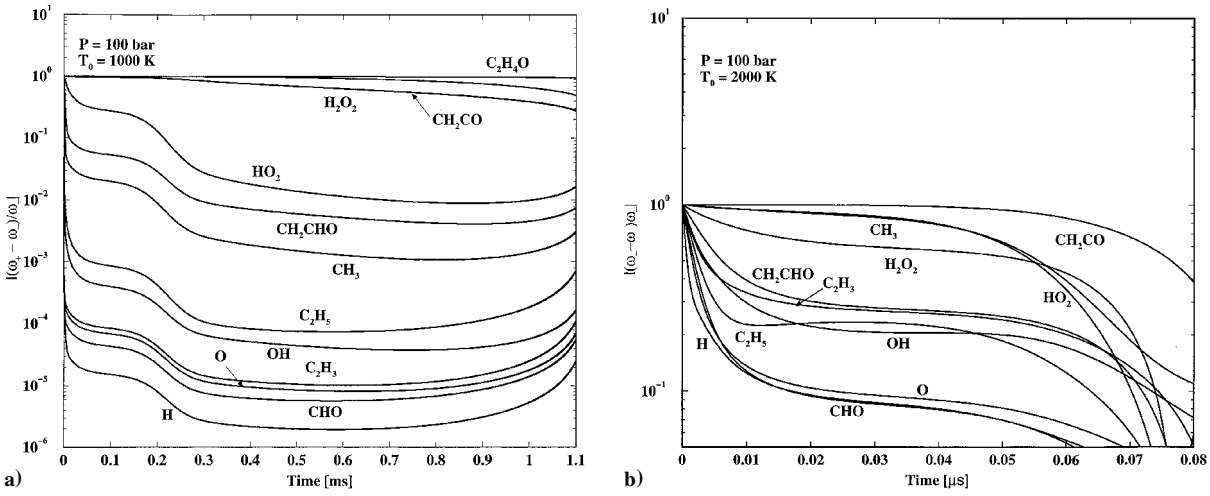

Fig. 7 Difference between the net forward and net backward reaction rates, divided by the net forward reaction rate, for various species in the adiabatic, isobaric evolution of stoichiometric ethylene–air mixtures at 100 bar and an initial temperature of a) 1000 K and b) 2000 K calculated from the detailed mechanism.

Fig. 6. They appear in the stoichiometry of the reduced chemistry of Table 2. Further reduction requires application of steady-state and partial-equilibrium approximations, which can lead to substantial savings in computation time.

Because the identity of the steady-state species depends strongly on initial temperature and pressure, to determine them it is helpful to plot histories of steady-state indicators. To exhibit such indicators, the evolution of the absolute value of the net production rate of each species, normalized by the forward production rate, is shown in Fig. 7 for a pressure of 100 bar and two initial temperatures of 1000 and 2000 K. At 1000 K, the species H, CHO, O, C_2H_3, OH, and C_2H_5 are seen to be in excellent steady state. In addition, CH_2CHO can be assumed to be in steady state, although at low temperatures this approximation is inaccurate. As temperature increases, the concentrations of radicals increase, and at 2000 K, only O, H, and CHO achieve good steady states. In addition, it was found that C_2H_5, CH_2CHO, and OH can be approximated by their steady-state concentrations at high temperatures without affecting ignition-time predictions significantly. Although H obeys a reasonably good steady state at high temperatures, this approximation is not introduced because its small unsteadiness is important for predicting C_2H_3 concentration histories at high temperatures.

From these results, it is seen that, for all temperatures and pressures of interest, O, CH_2CHO, CHO, C_2H_5, and OH can be assumed to be in steady state, a result that could have been used to reduce the 13-step nonlinear mechanism to 8 steps. As a consequence of these steady states, the corresponding radical concentrations can be expressed as

$$[\mathrm{O}] = \frac{\alpha_1[\mathrm{H}] + \alpha_{26}[\mathrm{C_2H_3}]}{\alpha_{18} + \alpha_{19}}$$

$$[\mathrm{CH_2CHO}] = \frac{\alpha_{19}[\mathrm{O}] + \alpha_{26}[\mathrm{C_2H_3}]}{\alpha_{29}}$$

$$[\mathrm{CHO}] = \frac{\alpha_{18}[\mathrm{O}] + \alpha_{25}[\mathrm{C_2H_3}]}{\alpha_{34} + \alpha_{35}}, \qquad [\mathrm{C_2H_5}] = \frac{\alpha_{22}[\mathrm{H}]}{\alpha_{30} + \alpha_{31}}$$

$$[\mathrm{OH}] = \frac{\alpha_1[\mathrm{H}] + 2\alpha_{11}[\mathrm{H_2O_2}] + \alpha_{20}[\mathrm{HO_2}] + \alpha_{27}[\mathrm{CH_3}]}{\alpha_{17}} \qquad (2)$$

These five steady-state approximations can be used to eliminate five reactions in Table 2 that consume these steady-state species, leading to a seven-step reduced mechanism, which can be written as follows.

Step I:

$$(16): \mathrm{C_2H_4 + O_2 \rightarrow C_2H_3 + HO_2}, \qquad \omega_I = \alpha_{16}[\mathrm{C_2H_4}]$$

Step II:

$$(25): \left.\begin{matrix} C_2H_3 \\ +\{1+(1-u)(s+q-qs)\}\,O_2 \\ +(1-s)C_2H_4) \end{matrix}\right\} \rightarrow \begin{cases} \{su+(1-s)(3+qu-2q)\}\,H \\ +(1-u)(s+q-qs)\,HO_2 \\ +q(1-s)\,CH_3 + s\,CH_2O \\ +(1-s)(2-q)\,CH_2CO \\ +(s+q-qs)\,CO \end{cases}$$

$$\omega_{II} = (\alpha_{25}+\alpha_{26})\,[C_2H_3]$$

Step III:

$$(20): 2\,C_2H_4 + 2HO_2 \rightarrow \begin{cases} C_2H_3 + H_2O + CH_3 \\ +CO + H_2O_2 \end{cases}$$

$$\omega_{III} = \alpha_{20}\,[HO_2]$$

Step IV:

$$(1): \left.\begin{matrix} \{1-pqu-2p(1-q)\}\,H \\ +\{1+pq(1-u)\}\,O_2 \\ +2p\,C_2H_4 \end{matrix}\right\} \rightarrow \begin{cases} \{1-p+pq(1-u)\}\,HO_2 \\ +p\,C_2H_3 + p\,H_2O \\ +pq\,CH_3 + pq\,CO \\ +p(1-q)\,CH_2CO \end{cases}$$

$$\omega_{IV} = (\alpha_1+\alpha_6)[H]$$

Step V:

$$(21): \left.\begin{matrix} r\,C_2H_4 \\ +\{r+t(1-r)\}\,H \\ +(1-r)t\,O_2 \end{matrix}\right\} \rightarrow \begin{cases} r\,C_2H_3 + r\,H_2 \\ +(1-r)t\,HO_2 \end{cases}$$

$$\omega_V = (\alpha_{21}+\alpha_{22})[H]$$

Step VI:

$$(27): CH_3 + O_2 + C_2H_4 \rightarrow CH_2O + C_2H_3 + H_2O$$

$$\omega_{VI} = \alpha_{27}[CH_3]$$

Step VII:

$$(11): 2C_2H_4 + H_2O_2 \rightarrow 2C_2H_3 + 2H_2O$$

$$\omega_{VII} = \alpha_{11}[H_2O_2]$$

where the numbers in parentheses on the left indicate the original reaction numbers with respect to Table 2, and ω_i represents the rates of these global reactions in terms of the rates of the elementary reactions in Table 1.

The first step in this reduced mechanism is the initiation step, which produces C_2H_3 and HO_2 and starts the ignition process; this step proceeds at the rate of the elementary initiation reaction 16 in Table 1. Like most initiation steps, this step is also endothermic, requiring about 250 kJ/mole of fuel consumed. The C_2H_3 radical reacts with O_2 and C_2H_4 to produce the active H and HO_2 radicals at the total rate of the elementary O_2 reactions with vinyl (reactions 25 and 26) in global step II. In addition to the active radicals, intermediates like CH_2O, CH_2CO, and CO are also produced in this overall step. This step is exothermic at low temperatures, releasing about 250 kJ, but at high temperatures it is slightly endothermic, consuming about 60 kJ.

Step III is important only below 1300 K and produces vinyl and methyl radicals at the rate of the elementary HO_2 attack on the fuel (reaction 20 in Table 1). Because of the high vinyl reactivity, this somewhat exothermic (heat release $Q = 183$ kJ) step is the primary radical-production step under low-temperature conditions. There is also a secondary branching path, step IV, which produces radicals at the total rate of the elementary H attack on O_2. The coefficient $\{1-pqu-2p(1-q)\}$ of H in this reaction is positive at low temperatures, for which p becomes small, thus rapidly transforming H into HO_2. As temperature increases, however, this coefficient becomes negative, because $p \rightarrow 1$, leading to the production of H along with HO_2 at the rate of the elementary reactions 1 and 6 in Table 1. This step is exothermic under all conditions, more so at low-temperature conditions, where it releases about 150 kJ, whereas it releases only 20 kJ at higher temperatures.

In step V, at high temperatures ($r \rightarrow 1$), the H radicals react with the fuel, leading to the production of vinyl at the rate of the elementary reaction 21 in Table 1. At low temperatures ($r \rightarrow 0$), however, this step produces HO_2 at the rate of the elementary reaction 22, and it effectively resembles elementary reaction 6 in Table 1. The energetics of this reaction also change with temperature, being exothermic ($Q = 175$ kJ) at low temperatures and endothermic ($Q = -15$ kJ) at higher temperatures. The usefulness of adopting reactant depletion as the ignition criterion at high temperatures is essentially due to the rapid consumption of fuel through this step.

Step VI is the oxidation of CH_3 into the relatively stable CH_2O and H_2O. This exothermic ($Q = 270$ kJ) step proceeds at the rate of the elementary O_2 attack on CH_3. The consumption of CH_3 can be neglected under most conditions, unless the energetics of this ignition process has to be considered. Finally, step VII ($Q = -118$ kJ), is the net radical production associated with the breakup of H_2O_2 at the rate of step 11 in Table 1.

Despite the simplicity of the seven-step reduced mechanism, the chemistry of ethylene ignition is quite complicated because it depends on the values of the parameters p, q, r, s, t, and u. The pressure and temperature dependences of these parameters, shown in Fig. 6, indicate two distinct regimes of ignition, where simplifying approximations can be made: the high-temperature regime, where the parameters $p \rightarrow 1$, $r \rightarrow 1$, $s \rightarrow 0$, $t \rightarrow 0$, and $u \rightarrow 1$, and the low-temperature regime where $p \rightarrow 0$, $r \rightarrow 0$, $t \rightarrow 1$, and $u \rightarrow 0$. The analysis of the seven-step mechanism is less involved if these simplifying approximations are introduced for these two limits.

High-Temperature Ignition

For high initial temperatures ($T_o > 1300$ K), the parameters s and t can be set to zero, and the parameter r can be set to unity. The parameters p, q, and u are allowed to vary with pressure and temperature to extend the range of our analysis. A simplified four-step reduced mechanism for high-temperature ignition is obtained after neglecting steps III, VI, and VII, which are unimportant for predicting ignition times under these conditions. From this four-step mechanism, a second-order linear inhomogeneous system is obtained for the active species C_2H_3 and H, namely,

$$\frac{d[C_2H_3]}{dt} = \alpha_{16}[C_2H_4] - \alpha_{26}[C_2H_3] + (\alpha_1+\alpha_{21})[H]$$

$$\frac{d[H]}{dt} = (3+qu-2q)\alpha_{26}[C_2H_3] + \{(1+qu-2q)\alpha_1 - \alpha_6 - \alpha_{21}\}[H] \quad (3)$$

These equations can be solved analytically, and concentration histories of C_2H_3 and H can be obtained. In terms of $\gamma \equiv \alpha_{21} - \alpha_1\{pqu + 2p(1-q) - 1\}$ and $\Delta \equiv \{(\gamma - \alpha_{26})^2 + 4\alpha_{26}(3+qu-2q)(\alpha_1+\alpha_{21})\}^{1/2}$, the eigenvalues $\lambda_{1,2}$, having concentrations proportional to $e^{\lambda t}$, are given by

$$\lambda_{1,2} = [-(\gamma+\alpha_{26}) \pm \Delta]/2 \quad (4)$$

where the positive eigenvalue λ_1 leads to the rapid exponential growth of $[C_2H_3]$ and [H], whereas the negative eigenvalue λ_2 is essentially insignificant because it provides a term in which the concentrations decay rapidly.

As discussed earlier, the ignition of ethylene under high-temperature conditions is due to rapid growth in the concentration of radicals, leading to reactant depletion. Thus, an expression for the ignition time can be obtained by identifying the onset of reactant depletion. This is approximately the time at which the concentrations of the radicals approach the concentrations of the reactants, that

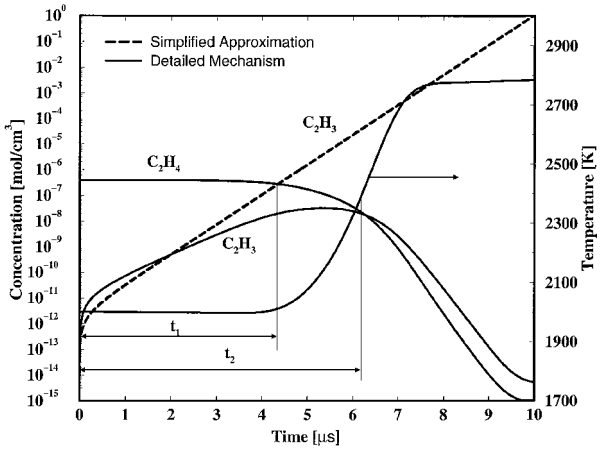

Fig. 8 Comparison of the C_2H_3 history from the detailed mechanism and from the prediction based on Eq. (3), for an initial temperature of 2000 K at 1 bar pressure.

is, when $[C_2H_3] \rightarrow [C_2H_4]$. Applying this criterion to the solution of Eq. (3), and using only the term that grows rapidly, leads to the expression

$$t_i = \frac{1}{\lambda_1}\ell n\left\{2\Delta\frac{(3+qu-2q)(\alpha_1+\alpha_{21})\alpha_{26}-\gamma(\alpha_{26}-\alpha_{16})}{\alpha_{16}(\Delta-\alpha_{26})(\Delta+\gamma+\alpha_{26})}\right\} \quad (5)$$

for the ignition time t_i. In this expression, λ_1 is proportional to $[O_2]$, independent of equivalence ratio ϕ, except for the contribution of $\alpha_{21} = (\frac{1}{3})k_{21}[O_2]\phi$.

The predictions using Eq. (5) are compared with the other predictions in Fig. 2. It is seen that, although the agreement is within a factor of two, the analytical expression always underpredicts the ignition time in comparison with the detailed mechanism. This can be understood from Fig. 8, where the concentration histories from the detailed mechanism are compared with those of the analytical result obtained by integrating Eq. (3). In Fig. 8, t_1 refers to the ignition time adopted for arriving at Eq. (5), whereas t_2 refers to the temperature-inflection criterion adopted for the predictions from the detailed mechanism. It is apparent that t_1 is lower than t_2 by a factor of 1.5–2.0, which accounts for the disagreement in Fig. 2.

Low-Temperature Ignition

A similar analysis can be carried out for low temperatures by setting the parameters p, u, and r to zero and the parameter t to unity. In addition, C_2H_3 and H are in excellent steady states, and their concentrations can be expressed as

$$[C_2H_3] = \frac{2\alpha_{11}[H_2O_2]+\alpha_{16}[C_2H_4]+\alpha_{20}[HO_2]+\alpha_{27}[CH_3]}{\alpha_{25}+\alpha_{26}}$$

$$[H] = \frac{(1-s)(3-2q)(\alpha_{25}+\alpha_{26})}{\alpha_6+\alpha_{22}}[C_2H_3] \quad (6)$$

These approximations lead to a four-step mechanism for ethylene ignition at low temperatures, which can be written as follows.

Step I:

$$\left.\begin{matrix}(2-s)C_2H_4\\ +\{5-q-s(2-q)\}O_2\end{matrix}\right\}\rightarrow\begin{cases}\{4-q-s(2-q)\}HO_2\\ +q(1-s)CH_3+sCH_2O\\ +(1-s)(2-q)CH_2CO\\ +(s+q-qs)CO\end{cases}$$

$$\omega_I = \alpha_{16}[C_2H_4]$$

Step III:

$$\left.\begin{matrix}(3-s)C_2H_4\\ +(1+s+(1-s)(3-q))O_2\\ +\{2s+q(1-s)-1\}HO_2\end{matrix}\right\}\rightarrow\begin{cases}(1+q-qs)CH_3+sCH_2O\\ +(1-s)(2-q)CH_2CO\\ +(1+s+q-qs)CO\\ +H_2O_2+H_2O\end{cases}$$

$$\omega_{III} = \alpha_{20}[HO_2]$$

Step VI:

$$\left.\begin{matrix}CH_3+\{5-q-s(2-q)\}O_2\\ +(2-s)C_2H_4\end{matrix}\right\}\rightarrow\begin{cases}\{3-q-s(2-q)\}HO_2\\ +q(1-s)CH_3+(1+s)CH_2O\\ +(1-s)(2-q)CH_2CO\\ +(s+q-qs)CO+H_2O\end{cases}$$

$$\omega_{VI} = \alpha_{27}[CH_3]$$

Step VII:

$$\left.\begin{matrix}(4-2s)C_2H_4+H_2O_2\\ +2\{4-q-s(2-q)\}O_2\end{matrix}\right\}\rightarrow\begin{cases}2(3-q-2s+sq)HO_2\\ +2q(1-s)CH_3+2sCH_2O\\ +2(1-s)(2-q)CH_2CO\\ +2(s+q-qs)CO+2H_2O\end{cases}$$

$$\omega_{VII} = \alpha_{11}[H_2O_2]$$

Under these conditions, the active species are HO_2 and H_2O_2. Step I is the initiation step, which produces HO_2 and leads to the production of H_2O_2 in the second step (step III). The third step (step VI) is energetically important but can be neglected for an initial analysis of the induction stage. The fourth step (step VII) leads to further production of HO_2 through the consumption of H_2O_2.

As explained in the Appendix, at low temperatures there is a constant-concentration stage following the chain-branching stage, during which radical–radical reactions cannot be neglected. To analyze this stage accurately, reaction 10 must be included, which removes HO_2, producing additional H_2O_2. This reaction can be included with the preceding steps to provide an improved but nonlinear four-step reduced mechanism for describing low-temperature ignition. A complete analysis would require solving the two evolution equations for $[HO_2]$ and $[H_2O_2]$. In view of the uncertainty in the low-temperature chemistry for ethylene, as explained in Part 1, it may be reasonable to achieve further simplification by introducing a steady-state approximation for H_2O_2. This will increase radical concentrations and thereby decrease predicted ignition times in comparison with those obtained from the present detailed mechanism. The balance equation for HO_2, after neglecting the relatively small contribution from step VI and applying the H_2O_2 steady state with k_{10} neglected, can then be written as

$$\frac{d[HO_2]}{dt} = [4-q-s(2-q)]\,\alpha_{16}[C_2H_4]$$
$$+[7-6s-3q(1-s)]\alpha_{20}[HO_2]-k_{10}[HO_2]^2 \quad (7)$$

An expression for the steady-state concentration of HO_2 in the constant-concentration stage can be obtained from Eq. (7) after neglecting the small contribution of the initiation step, resulting in the expression

$$[HO_2] = \frac{[7-6s-3q(1-s)]\alpha_{20}}{k_{10}} \quad (8)$$

Equations (2), (6), and (8) can then be used to obtain the concentrations of all intermediates at the onset of the constant-concentration stage. The time for ignition under low-temperature conditions can be written as $t_i = t_{cb} + t_{cc}$, where t_{cb} refers to the duration of the chain-branching stage and t_{cc} refers to the duration of the constant-concentration stage. An expression for t_{cb} can be derived by identifying the time at which $[HO_2]$ reaches the value given by Eq. (8), and this leads to the equation

$$t_{cb} = \frac{1}{[7-6s-3q(1-s)]\alpha_{20}}$$
$$\times\ell n\left(1+\frac{\alpha_{20}^2[7-6s-3q(1-s)]^2}{\alpha_{16}[C_2H_4]k_a[4-q-s(2-q)]}\right) \quad (9)$$

which gives about one-eighth the value obtained with the detailed mechanism, for which H_2O_2 is not in steady state. To obtain an expression for t_{cc}, thermal-explosion theory can be applied, with the exothermic global step III ($Q = 600$ kJ) plus step VII ($Q = 730$ kJ), releasing about 1300 kJ, leading to thermal runaway. Such an expression is not expected to be very accurate, however, because the influences of the additional overall step VI and elementary reaction $HO_2 + OH \rightarrow H_2O + O_2 + 295$ kJ are not entirely negligible. In view of these complications and the limited usefulness of such an expression, this analysis is not carried further here.

Detonation Chemistry

The induction zone is followed by several stages of heat release, the chemistry of which is quite different from the induction-zone chemistry because radical–radical and intermediate-radical reactions, rather than reactant-radical reactions, are very active. These stages begin right after the induction zone and end when the final conditions are attained. Although the final conditions can be nonequilibrium in particular experiments, because of influences of slow chemical steps, in practice complete chemical equilibrium usually is a good approximation to the final state. With radiant and convective energy losses neglected, this equilibrium state is determined uniquely by the initial state through the conservation laws and adiabaticity condition, independently of the chemical-kinetic history.

For all initial conditions, the first stage of postinduction heat release begins when the methyl radicals are oxidized. This starts toward the end of the induction zone through the elementary step 27 in Table 1 but because of the rapid buildup of the O-atom concentration at the end of ignition, it proceeds largely through step 28 in Table 1, which releases about 290 kJ of heat and is followed by the formaldehyde oxidation step 33, $CH_2O + OH \rightarrow CHO + H_2O + 122$ kJ. There is additional production of CH_3 through the oxidation of ketene by $CH_2CO + H \rightarrow CH_3 + CO + 140$ kJ (step 32), which along with the reaction $CHO + H \rightarrow CO + H_2 + 375$ kJ, step 36, is important for fuel-rich conditions, where it releases additional heat and leads to the formation of CO. The HO_2 consumption reactions (reactions 7–9 in Table 1) and the formation and consumption of acetylene through reactions 24 and 37 are likewise important for fuel-rich conditions, but can safely be neglected for lean or stoichiometric mixtures. The hydrogen–oxygen shuffle reactions, steps 2–5 in Table 1, are important for fuel-lean conditions. All of these additional stages of heat release occur rapidly, right after the induction period, contributing to the steep increase in temperature.

This sharp temperature increase is followed by the CO oxidation stage, where the reactions 14 and 15 in Table 1 are important. At high temperatures, CO_2 dissociates to CO, whereas at low temperatures, CO is oxidized to CO_2, releasing heat. The CO chemistry is slower than the steps identified earlier, but faster than radical recombination. The slow radical-recombination stage, during which H and OH recombine to produce H_2O, is the final stage of the detonation. This stage proceeds at the rate of the radical-recombination reaction 12, which is the principal recombination, retained here as representative of all recombinations and which requires the reverse step 13 to achieve chemical equilibrium.

The analysis of the preceeding section and discussion leads to the possibility that a two-step mechanism for ethylene–air detonations can be constructed. In our earlier work on acetylene detonations,[8] a seven-step reduced mechanism for high-temperature acetylene detonations was developed. Out of these seven steps, only four were important during induction, and the remaining three steps released heat at different rates after the induction period. As a simplification, the four steps were combined into one single step to model the ignition process, and the remaining three steps were combined into a single step to model the slow heat release. Such a systematic reduction to a two-step mechanism cannot be performed for ethylene detonations because of the inapplicability of a large number of steady-state approximations, especially at high temperatures. For this reason, a more semi-empirical approach is adopted here. High-temperature conditions are emphasized, with ignition-time errors as large as a factor of 10 accepted at the lowest temperatures.

The first step in the two-step ethylene mechanism produces intermediates, radicals, and heat at a rate that is the sum of an initiation rate and a branching rate. The identities of the species in this step are established by analyzing the concentration histories using the detailed mechanism and identifying the species that are in high concentrations at the end of the induction period. The species CO and H_2O were found in this way to be the main products at the end of the induction period. Although CH_3 and CH_2CO are also produced, as seen in the reduced mechanism, these intermediates are consumed rapidly through the elementary reactions in Table 1, producing CO and H_2O. It is also clear from the reduced mechanism that H is the most important non-steady-state active species during the induction period; OH is also produced in high concentrations, especially right after ignition.

From these results, a general one-step approximation for the ignition stage can be written as $C_2H_4 + \{2 - (f_1 - f_2)/4\}O_2 \rightarrow 2CO + \{2 - (f_1 + f_2)/2\}H_2O + f_1H + f_2OH$, where f_1 and f_2, respectively, refer to the number of moles of H and OH produced in the induction zone per mole of fuel consumed. After initiation, this reaction proceeds at a branching rate that depends, in particular, on the rate of the elementary reaction 1 in Table 1. Analogous to acetylene (Ref. 8), reaction 1 is selected to represent the overall branching. The values for f_1 and f_2 are to be chosen to predict temperature histories that lead to good agreement with those obtained from the detailed mechanism. The main quantities to be predicted well are the ignition time and the heat released in the induction stage.

Because of the selection of the elementary reaction 1, the parameter f_1 is most important for the ignition time; after f_1 is chosen, the value of f_2 affects the heat release. For acetylene, $f_1 = f_2 = \frac{1}{2}$ is preferred.[8] For ethylene, the choice $f_1 = f_2 = \frac{2}{3}$ provides the best agreement for temperature histories under the conditions of interest; like acetylene, this has $f_1 = f_2$. A one-step approximation for the ignition process, thus, can be written as follows.

Step A:

$$C_2H_4 + 2O_2 \rightarrow 2CO + \tfrac{4}{3}H_2O + \tfrac{2}{3}H + \tfrac{2}{3}OH + 424\ \text{kJ}$$

with the rate

$$\omega_A = k_{14}[C_2H_4][O_2] + p'k_1[H][O_2]H\{[C_2H_4]\} \qquad (10)$$

where the parameter $p' = k_1/(k_1 + k_6[M] + tk_{22})$ and $H\{\}$ denotes the Heaviside step function, unity until $[C_2H_4]$ approaches zero and zero thereafter. The parameter p' has been introduced as a modified version of the parameter p to extend the range of applicability of the two-step mechanism. When the temperature decreases, the global reaction V, which proceeds at the rate of elementary reaction 22, contributes to the elementary reaction 6 and, hence, the value of p' tends to be lower than p. The factor $H\{\}$ has been introduced to turn off the branching after the fuel is depleted.

Establishing the identity of the products and rates for the second step is straightforward. As explained previously,[8] the requirement is that CO and CO_2 be in equilibrium through the steps 14 and 15 and that the equilibrium of the recombination reactions 12 and 13 not be violated. This leads to the second step for the two-step mechanism, which can be written as follows.

Step B:

$$2CO + \tfrac{4}{3}H_2O + \tfrac{2}{3}H + \tfrac{2}{3}OH + cO_2 \rightleftharpoons (2-a)\,CO_2 + a\,CO + (2-b)H_2O + 2b(OH + m\,H)/(1+m)$$

where $m \equiv [H]_\infty/[OH]_\infty$, $n \equiv k_{12\infty}[H_2O]_\infty/k_{13\infty}$, and

$$a = \frac{2}{1 + k_{14\infty}/(mk_{15\infty})}, \qquad b = \frac{2(1+m)}{1 + m + 2\sqrt{mn}}$$

$$c = \frac{(2-a)}{2} + \frac{b(1-m)}{2(1+m)} \qquad (11)$$

The rate of this reaction is given by

$$\omega_B = \tfrac{3}{2}(k_{12}[M][H][OH] - k_{13}[M][H_2O]) \qquad (12)$$

Reactions A and B, just shown, along with the rates given by Eqs. (10) and (12), constitute the two-step mechanism that may be applied to ethylene ignition in air.

Calculations made with steps A and B result in good agreements with those from the detailed mechanism, as shown in Figs. 2 and 3. Although at the lower pressures the two-step results in Fig. 3 for the heat release subsequent to ignition differ noticeably from the more accurate results, there is virtually no practical interest in this part of the profile at 1 bar or below because detonation pressures are higher; this approximation was selected with this observation in mind. Even for off-stoichiometric conditions, the agreement with the detailed mechanism was found to be reasonable. In deriving the two-step mechanism, we have assumed that the first step is chain branching and also exothermic. Calculations with the detailed mechanism, however, indicate that the chain-branching stage is actually endothermic, at least initially, leading to the production of CH_3 and CH_2CO. This causes a drop in temperature by amounts from a few degrees to 50 deg at the highest initial temperatures. The conversion of CH_3 and CH_2CO to CH_2O and CO, however, takes place almost immediately at the end of induction, releasing heat and leading to exothermic induction being a reasonable approximation. Our choice of CO and H_2O as the products at the end of the induction period is an approximation designed to retain the main influences of all of these processes as simply as possible.

Conclusions

Attention has been devoted to ethylene ignition and detonation, limited to the range of conditions addressed in Part 1. A short mechanism for ethylene autoignition and detonation has been identified that retains the essence of the chemical pathways and that yields reasonably accurate results, giving ignition times that differ from those of the detailed mechanism by less than 30% for ignition in air. On the basis of this short mechanism, a seven-step reduced mechanism has been developed for ignition under all conditions of interest. This seven-step mechanism simplifies under low-temperature and high-temperature conditions, and expressions for ignition times are given for high-temperature conditions that produce agreement with predictions from the detailed mechanism within a factor of two. From the understanding gained in the systematic reduction, a simplified two-step description has been developed for detonation, part of which is a one-step description for ignition that produces excellent agreement with the detailed mechanism at the highest temperatures considered but underpredicts ignition times by as much as an order of magnitude at the lowest temperatures considered.

When these degrees of agreement are kept in mind, the present results can be applied with some confidence between equivalence ratios of 0.5 and 2.0 and initial (postshock) temperatures between 1000 and 2500 K, for pressures between 0.1 and 10 bar. At the higher pressures of interest, up to 100 bar, additional uncertainties arise mainly from uncertainties in the detailed mechanism. Especially for the lower temperatures at these high pressures, uncertainties in the extent of chain branching engender corresponding uncertainties in the present results. It is prudent to recognize these uncertainties and limitations, even though results obtained through systematic reduction may be expected to be more robust than purely empirical correlations.

Appendix: General Characteristics of the Induction Zone

Further details of the initiation, chain-branching and constant-concentration stages may be of interest, especially in comparison with induction-zone characteristics of other fuels.

Initiation Stage

Because no radicals are present initially, an initiation stage is essential in the ignition mechanism. Many treatments, nevertheless, ignore this stage, arbitrarily assigning small but nonzero values to initial radical concentrations. This avoids the necessity of addressing initiation steps, but also prevents dependences on rates of elementary initiation steps from being determined. These dependences are weak but usually not entirely negligible; they would be negligible if ignition occurred in a constant-concentration stage that was long compared with the chain-branching stage, but this does not apply for ethylene over the conditions investigated here. The radical concentrations emerging from the initiation stage affect the duration of the chain-branching stage, which in turn affects the ignition time. If the ignition time is dominated by the duration of the chain-branching stage, the longest stage for ethylene at higher temperatures, excluding postignition processes, then the ignition time depends noticeably on initiation rate parameters because it is proportional to the logarithm of the reciprocal of the radical concentrations at the end of the initiation stage. For branched-chain thermal explosions, the dependence of the ignition time on initiation rates also is logarithmic.[12] It is concluded from these considerations that initiation rate parameters do affect ethylene ignition times.

There is a parallel between the initial initiation steps for ethylene and methane. For methane, below 1300 K the first step is $CH_4 + O_2 \rightarrow CH_3 + HO_2$, whereas the step $CH_4 + M \rightarrow CH_3 + H + M$ begins to be significant at higher temperatures, contributing to a higher effective overall activation energy for the ignition time of methane at higher temperatures (a characteristic not shared by the ignition of other hydrocarbon fuels[11,14]). For ethylene, from Table 1, the first step, similarly, is mainly $C_2H_4 + O_2 \rightarrow C_2H_3 + HO_2$, with $C_2H_4 + M \rightarrow C_2H_3 + H + M$ not becoming important until higher temperatures ($T > 2000$ K) and having an activation energy lower than that of methane dissociation so that an associated change in the effective overall activation energy for the ethylene ignition time does not occur. Acetylene, incidentally, is different, the O_2 affinity being comparatively large and the H abstraction and dissociation negligible in comparison, so that $C_2H_2 + O_2 \rightarrow$ products other than $C_2H + HO_2$ is the first step.[8] These different hydrocarbons, thus, behave differently in the initiation stage.

Subsequent steps in the initiation stage for ethylene with the mechanism investigated are mainly steps 20, 17, 25, and 26 of Table 1. These steps are analogous to the steps $CH_4 + HO_2 \rightarrow CH_3 + H_2O_2$ and $CH_3 + O_2 \rightarrow CH_2O + OH$ during methane initiation,[11] although the very reactive vinyl radical plays a proportionally greater role for ethylene than methyl does for methane; the greater reactivity of vinyl is, in fact, a principal reason that ignition times for ethylene are much shorter. Similar to methane, however, in the initiation stage, the concentrations of HO_2 and C_2H_3 initially increase linearly with time, whereas the concentration of formaldehyde initially increases quadratically with time. The O atom from step 26 enables steps 18 and 19 to begin, so that the methyl concentration initially increases cubicly with time, as does the H-atom concentration, from steps 19 and 29, both following from step 26, as well as from step 34, which follows from step 25 and from step 33. Following step 20 of Table 1, the hydroxyl radical generated increases initially cubicly, but less strongly than the quartic increase through step 1 or, at low temperatures, through steps 38 and 11. The OH enables step 17 to begin, and the H steps 21 and 22. Steps 29, 34, and 35 are rapid, so that ketene, CO, and additional radicals appear; the first of these stable species, for example, play a role similar to that of formaldehyde in the methane mechanism but initially increase cubicly rather than quadraticly with time. The active radicals that may achieve steady states during the initiation stage include CH_2CHO, CHO, O, OH, C_2H_3, and H. The first three of these in fact attain good steady states, but the others are poorer, thereby affecting subsequent descriptions of the chain-branching stage. In particular, at high temperatures the formation of C_2H_3 and H through steps 21 and 29, respectively, is too fast for these species to attain good steady states.

From observations such as this, a detailed mathematical description of the history of the initiation stage can in principle be developed, similar to that presented for methane for temperatures below 1300 K (Ref. 11). The complete ethylene analysis would, however, be considerably more complicated because of the larger number of active radicals, despite the simplifications that arise from the present

system being predominantly linear. Numerical rather than analytical approaches, therefore, are favored.

Chain-Branching Stage

The chain-branching stage begins after the steady states identified earlier are reached. In discussing this stage, for simplicity, steps 22, 23, 24, 30, 31, and 37 of Table 1 (also see Ref. 15), which are of lesser importance, are omitted here, as are steps 12–15, which become significant only in the later heat-release stage. Radical concentrations are still small enough that radical–radical reactions remain negligible, and the initiation step 16 is no longer of importance. In addition, steps consuming most other nonradical species not present initially, namely, CH_2CO, CH_2O, CO, H_2, and H_2O, are negligible because the concentrations of these species have not yet increased to levels at which their interactions with radicals are important. With these deletions, only steps 1, 6, 11, 17–21, 25–27, 29, 34, 35, and 38 are relevant during this stage.

These 15 elementary steps operative during the chain-branching stage in this level of description have an important feature in common, namely, that, except for step 38 important only at the lowest temperatures, they form a linear system, as indicated earlier. Analytical solutions of the kind developed there, therefore, are possible; in that respect, ethylene is simpler than methane, which is nonlinear.[11] Although the system with the 15 elementary steps is of the 11th order, under restricted ranges of conditions significant simplifications can be introduced, leading to analytical solutions, as seen earlier. These analytical solutions are advantageous in that they exhibit explicitly the dependences on specific reaction-rate constants and reactant concentrations, unambiguously identifying the exact roles played by the various elementary steps.

Constant-Concentration Stage

In our investigations of other fuels, we have not found the particular kind of constant-concentration stage that occurs at the lower temperatures with the mechanism studied here for ethylene. It is brought about by the onset of nonlinearity associated with HO_2 approaching a steady state. Although step 20 of Table 1 consumes HO_2, this consumption is insufficient to balance the production rate by steps 6 and 35. After concentrations have increased to a point at which radical–radical reactions become important, however, steps 7–9 enter, and more especially step 10, causing the growth of the HO_2 concentration to level off, so that the HO_2 concentration approaches a constant value. The resulting recombination terminates branching, so that all species concentrations cease to increase exponentially with time. It would be of interest to investigate whether HO_2 can play a similar role in induction processes for other fuels.

Acknowledgments

This work was supported by the Office of Naval Research through Contract N00014-99-1-0745. The authors would like to thank S. C. Li for his contribution during the initial stages of this work.

References

[1] Jachimowski, C. J., "An Experimental and Analytical Study of Acetylene and Ethylene Oxidation Behind Shock Waves," *Combustion and Flame*, Vol. 29, No. 1, 1977, pp. 55–66.

[2] Westbrook, C. K., Dryer, F. L., and Schug, K. P., "Numerical Modeling of Ethylene Oxidation in Laminar Flames," *Combustion and Flame*, Vol. 52, No. 3, 1983, pp. 299–313.

[3] Dagaut, P., Boettner, J. C., and Cathonnet, M., "Ethylene Pyrolysis and Oxidation—A Kinetic Modeling Study," *International Journal of Chemical Kinetics*, Vol. 22, No. 6, 1990, pp. 641–664.

[4] Marinov, N. M., and Malte, P. C., "Ethylene Oxidation in a Well-Stirred Reactor-Stirred Reactor," *International Journal of Chemical Kinetics*, Vol. 27, No. 10, 1995, pp. 957–986.

[5] Hidaka, Y., Nishimori, T., Sato, K., Henmi, Y., Okuda, R., and Inami, K., "Shock-Tube and Modeling Study of Ethylene Pyrolysis and Oxidation," *Combustion and Flame*, Vol. 117, No. 4, 1999, pp. 755–776.

[6] Wang, H., and Frenklach, M., "A Detailed Kinetic Modeling Study of Aromatics Formation in Laminar Premixed Acetylene and Ethylene Flames," *Combustion and Flame*, Vol. 110, No. 1–2, 1997, pp. 173–221.

[7] Wang, W., and Rogg, B., *Reduced Kinetic Mechanisms for Applications in Combustion Systems*, edited by N. Peters and B. Rogg, Vol. m15, Lecture Notes in Physics, Springer-Verlag, Berlin, 1993, Chap. 6, pp. 76–101.

[8] Varatharajan, B., and Williams, F. A., "Chemical-Kinetic Descriptions of High-Temperature Ignition and Detonation of Acetylene-Oxygen-Diluent Systems," *Combustion and Flame*, Vol. 124, No. 4, 2001, pp. 624–645.

[9] Varatharajan, B., and Williams, F. A., "Ethylene Ignition and Detonation Chemistry," *Journal of Propulsion and Power*, Vol. 17, No. 6, 2001.

[10] Pitsch, H., "Entwicklug eines Programmpaketes zur Berechnung eindimensionaler Flammen am Beispeil einer Gegenstomdiffusionsflamme," M.S. Thesis, RWTH Aachen, Inst. für Technishe Mechanik, Aachen, Germany, Jan. 1993.

[11] Li, S. C., and Williams, F. A., "Reaction Mechanisms for Methane Ignition," *Journal of Engineering for Gas Turbines and Power*, 2001 (to be published); also American Society of Mechanical Engineering, ASME Paper 2000-GT-0145.

[12] Varatharajan, B., and Williams, F. A., "Ignition Times in the Theory of Branched-Chain Thermal Explosions," *Combustion and Flame*, Vol. 121, No. 1/2, 2000, pp. 551–554.

[13] Williams, F. A., *Combustion Theory*, 2nd ed., Addison–Wesley, Redwood City, CA, 1985, pp. 576–581.

[14] Colket, M. B., III, and Spadaccini, L. J., "Scramjet Fuels Autoignition Study," *Journal of Propulsion and Power*, Vol. 17, No. 2, 2001, pp. 315–323.

[15] Feng, Y., Niiranen, J. T., Bencsura, A., Knyazev, V. D., and Gutman, D., "Weak Collision Effects in the Reaction C2H5 = C2H4 + H," *Journal of Physical Chemistry*, Vol. 97, No. 4, 1993, pp. 871–880.